



# Microencapsulation of a coconut oil-based alkyd resin into poly (melamine–urea–formaldehyde) as shell for self-healing purposes



Saied Nouri Khorasani\*, Shahla Ataei, Rasoul Esmaeely Neisiany

Department of Chemical Engineering, Isfahan University of Technology, Isfahan 84156-83111, Iran

## ARTICLE INFO

### Keywords:

Coconut oil  
Alkyd resin  
Microencapsulation  
Poly(melamine-urea-formaldehyde)  
Self-healing

## ABSTRACT

In the present study, a coconut oil-based alkyd resin was successfully encapsulated into poly (melamine-urea-formaldehyde) (PMUF) as shell material using sodium dodecyl benzene sulfonate (SDBS) as an emulsifier. The influence of encapsulation processing conditions such as melamine resin/urea (M/U) ratio, initial pH value of medium and mechanical agitation rate on encapsulation yield and core content were studied. Chemical structure, thermal stability, size distribution and surface morphology of microcapsules were characterized by Fourier transform infrared (FTIR) spectroscopy, optical and scanning electron microscopy (SEM), and thermal gravimetric analysis (TGA) respectively. The produced microcapsules at optimum processing condition were white and free-flowing spherical particles. The encapsulation yield and core content of synthesized microcapsules were controlled by selecting various processing condition. The rough outer surface of microcapsules was agglomerated PMUF nanoparticles which would provide better adhesion to matrix.

## 1. Introduction

The economic impact of corrosion of metallic structures in aggressive environments is a major concern for all industries globally. One approach to prevent corrosion is to apply polymeric coatings on metallic structures. On many situations, cracks occur on the surface of coatings which can disturb the protection process and in some cases could lead to a situation worse than bare surfaces. The application of protective polymeric coatings that act as a barrier against corrosive species is the most common and cost-effective method of improving corrosion resistance behavior, and therefore the durability of metallic structures [1].

Self-healing materials as an organic coating have been proposed to prolong metallic material life against corrosion and recover its initial properties after cracking due to the external environment or internal stresses. Therefore in a self-healing coat, healing occurs where micro-crack initiates and protects the crack from propagation and decreases penetration of oxygen, water, and ions down to the substrate. In many recent years, many attempts have been made to produce an optimized self-healing material using microcapsules containing healing agent, especially in coating industries. Several selected healing agents have been successfully encapsulated for using in epoxy resins as matrix, such as dicyclopentadiene (DCPD) [2], oil soluble solvents [3], linseed oil (LO) [4], tung oil [5], epoxy and amine [6–8], mercaptan [9–11], and alkyd resins [12,13]. In designing a microcapsules-based self-healing

system, various important factors should be taken into account. All these systems use a liquid healing agent as a core that must be inert to the polymeric shell, and also, microcapsules should be compatible with the host matrix [6].

Alkyd resins are relatively inexpensive to produce and has excellent properties such as high gloss, acceptable color retention, and excellent thermal stability. These properties make them suitable for a broad range of applications such as paint, adhesive, ink, varnish and various coating industries, by changing the oil length, type of the unsaturated oil, and chemically modifications [14,15]. Alkyd resins have been synthesized via polycondensation reaction of polyhydric alcohols and polyacids modified with triglyceride oils. Fig. 1 displays a plausible simple structure of the alkyd resins. Alkyds are versatile materials and can be designed such to have specified amount of carboxyl and hydroxyl groups as crosslinking sites. In addition to the properties mentioned above, the viscosity of alkyd resin can be changed in the formulation without adding diluent to make them more suitable as healing agents. Moreover, when alkyd resin flows into the crack plane on the matrix, does not cause toxic fumes such as those aprotic solvent-based self-healing systems [16].

Vegetable oils are reasonably inexpensive, safe to work with, and eco-friendly. These reasons made them easy to use in high-performance anticorrosive coatings in large scale uses in various industries. Due to the presence of unsaturated fatty acids in LO and tung oil [5], these oil's molecules tend to crosslink with oxygen to make a stable complex and

\* Corresponding author.

E-mail address: [saied@cc.iut.ac.ir](mailto:saied@cc.iut.ac.ir) (S.N. Khorasani).

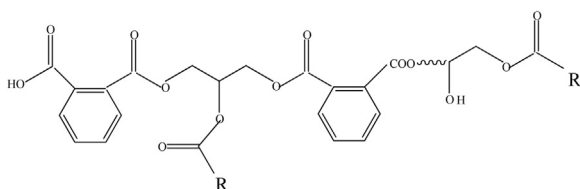


Fig. 1. A plausible structure of the alkyd resin, where R stands for fatty acid in triglyceride oil.

finally a waterproof surface. Coconut oil as a non-drying oil has some saturated fatty acids, and as compared with LO and tung oil in Table 1, there is not a lot of unsaturation in its structure. For centuries, this oil has been used in paints and coatings.

It should be mentioned, to modify properties of a particular resin, usually for coating applications, alkyd, and epoxy resins are blended (physically or chemically). Dutta et al. [17], reported coatings with suitable drying time, hardness, gloss, and flexibility by blending a Nahar seed oil-based alkyd with epoxy. Palm oil-based alkyd resin was blended with epoxy by Issam et al. [18] and Ong et al. [19] to improve the performance as a potential coating. Assanvo et al. [20] used ricinodendronheudelotii oil-based alkyd resin and blended it with epoxy resin for coating applications. Gogoi et al. [21] used a Jatropha curcas oil-based alkyd/epoxy blends as bio-reinforced composites for various applications. Lee et al. [22] and Khong & Gan, [23] reported that palm oil-based alkyds were compatible with epoxidized natural rubber which in turn could modify the properties of rubber compounds. All these studies showed good compatibility between alkyd and epoxy resin.

Therefore in subsequent research, crosslinking reaction of carboxyl and hydroxyl functional groups in coconut oil-based alkyd resin proposed as a healing reaction in the epoxy matrix. The related reactions between functional groups in alkyd structure with epoxy resin have been shown by Shahabudin et al. [13]. The aforementioned reaction reveals the difference between the alkyd and vegetables oils such as LO and tung oil in healing mechanism.

Urea-formaldehyde (UF) resin widely used for the synthesis of microcapsules shell to protect the healing agents to prevent its spontaneous mixing with the matrix material during processing or storage. Microcapsules with PMUF shell are rigid and easier to handle than those only with PUF as the shell. Liu et al., modified PUF resin by mixing urea with MF prepolymer forming poly (melamine-urea-formaldehyde) (PMUF) in encapsulating 5-ethylidene-2-norbornene [24]. Tong and co-researchers replaced up to 12 Wt.% of urea with melamine in the formulation, to encapsulate epoxy resin. They reported that the PMUF microcapsules performed better resistance to solvents, acids, and alkalis [25]. Due to the higher functionality, melamine resin-formaldehyde networks are more rigid and show a higher heat resistance properties than UF resin [26]. Then et al. had encapsulated DCPD, using a small amount of melamine resin, in shell formulation materials [27]. The produced microcapsules were rigid enough to tolerate mixing condition with a viscous restorative dental resin.

Although there are several procedures in encapsulation [28], these techniques must be suitable to satisfy the various demands of particular self-healing material. Up to now, most capsules used in self-healing materials are prepared by in situ or interfacial polymerization in an oil-in-water emulsion system. In the second method, despite having

many benefits, the resulting microcapsules generally possess certain unreacted shell monomers, which can react with the core material and potentially cause to deactivate the core material [28]. In situ polymerization requires longer reaction times compared with other encapsulation techniques. However, this method offers some advantages such as low costs and ease of industrialization and simplicity of the procedure.

In this study, our aim is to encapsulate a coconut oil-based alkyd in PMUF microcapsules via in situ polymerization into an oil-in-water emulsion. The PMUF microcapsules consisting of coconut oil-based alkyd were characterized by Fourier transform infrared (FTIR) spectroscopy, optical (OM) and scanning electronic microscopy (SEM), and thermogravimetric analysis (TGA) to investigate their chemical structure, size distribution, surface morphology and thermal stability respectively.

## 2. Experimental

### 2.1. Materials

Coconut oil-based alkyd resin (ALK) with viscosity 5.6 stocks ( $5.6 \times 10^{-4} \text{ m}^2/\text{s}$ ), acid value  $6 \text{ mg KOH g}^{-1}$  and oil length% 62 was purchased from Aria Resin Co., Iran. Urea (U) was provided by Tianjin chemical plant, China. Ammonium chloride, hydrochloric acid, sodium hydroxide, polyvinyl alcohol (PVA) ( $M_w 61000 \text{ g/mol}$ ) and 1-octanol were obtained from Sigma-Aldrich, while formaldehyde (F) (37% aqueous) was provided by Pars Chemie Co., Iran. Melamine resin (Cymel 303<sup>®</sup>) (M), was supplied by coating Industries, Iran. 1, 3-dihydroxybenzol (resorcinol) was purchased from Merck, and sodium dodecylbenzene sulfonate (SDBS) (60% purity), used as an emulsifier, were purchased from Daejung Chemicals and Metals Co, Korea. All materials and chemical were used as received without any further purification.

### 2.2. Preparation of PMUF microcapsules (Encapsulation)

The PMUF microcapsules were prepared through one step in situ polymerization in an oil-in-water emulsion based on the method explained in the literature (with some modifications) [2]. At room temperature, an aqueous solution was prepared by dissolving 0.635 g of SDBS in 135 mL of deionized water in a 400 mL beaker, which was suspended in an oil bath on a programmable hot plate. The solution was agitated using a digital mixer that drove a 60 mm diameter stainless steel four-bladed, low-shear mixing propeller which was placed just above the bottom of the beaker. 10 g of ALK was slowly added to the aqueous solution to form emulsion stirring at 250 rpm for 15 min. Then specified amount of U and Cymel 303<sup>®</sup> (M) were added to the agitating emulsion, followed by addition of 0.25 g ammonium chloride and 0.25 g resorcinol. The Cymel 303<sup>®</sup> (~25 to 40 drops) was dissolved in a minimum quantity of ethanol before it was added to the beaker. Then, the emulsion was allowed to stabilize for further 20 min at the same agitation rate. Subsequently, the emulsion was adjusted to designated pH by adding a few drops of 10% sodium hydroxide and 1 M hydrochloric acid.

Finally, 6.35 g of formaldehyde solution and a few drops of 1-octanol as antifoaming agent were added to the mixture. The emulsion was covered with aluminum foil and slowly heated to 57 °C. During the period of reaction, as the temperature increased, the appearance of

Table 1  
Weight percentage of major saturated and unsaturated fatty acids in linseed oil, tung oil and coconut oil [29].

Oil	Linolenic C18:3	Elostearic C18:3	Linoleic C18:2	Oleic C18:1	Palmitic C16:0	Myristic C14:0	Lauric C12:0	Decanoic C10:0	Caprylic 7:0	Other
Linseed	52	–	16	22	6	–	–	–	–	4
Tung	3	80	4	8	5	–	–	–	–	–
Coconut	–	–	–	6.5	9.5	16	48	8	7	5

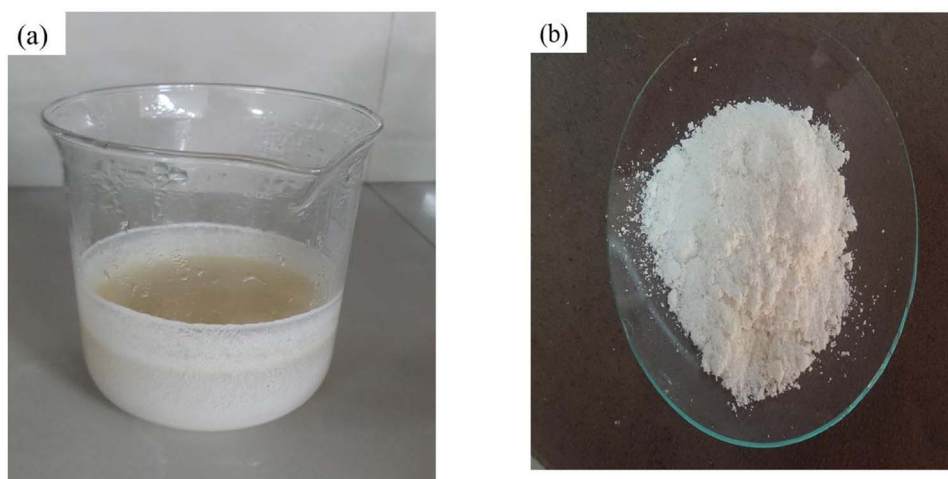


**Fig. 2.** (a) Final slurry after the synthesis of PMUF/ALK microcapsules which was washed, filtered, and dried to obtain (b) the produced microcapsules in the form of a free-flowing white powder.

solution initially became a cloudy emulsion. The reaction completed with the formation of a milky white suspension slurry containing microcapsules, after 4 h of continuous agitation. Then final suspension slurry was allowed to cool down to ambient temperature.

The ALK-filled microcapsules were floated at the top of the reactor, while the bigger PMUF particles settled down to the underneath of the water and at the bottom of the reactor (Fig. 2a). The residual white solid matter was separated from microcapsules by decantation method from the suspension after the synthesis. Afterward, product was collected on the filter paper. Subsequently, obtained microcapsules were washed several times with distilled water to remove unreacted chemicals, finally rinsed with ethanol twice and dried at ambient temperature for 24 h. Fig. 2b shows the produced microcapsules in the form of a free-flowing white powder.

The preparation of product was also carried out in the absence of ALK under the same experimental conditions, to characterize of the neat PMUF.

### 2.3. Characterization

#### 2.3.1. Chemical structure investigation by FTIR

The chemical structures of the ALK (as core), PMUF (as shell) and microcapsules were separately investigated. A WQF-510A China, Fourier transform infrared spectrometer (FTIR) at room temperature, with 32 scans from 4000 to 400  $\text{cm}^{-1}$  at the resolution of 4  $\text{cm}^{-1}$  were used. The samples of the shell material and microcapsules containing ALK were prepared by grinding with KBr, while a thin layer of the ALK and core extracted samples were separately spread onto the sodium chloride cell (NaCl pellet technique).

#### 2.3.2. Calculation of encapsulation yield and core content

The yield of the product was calculated from the weight of the dried microcapsules over the total weight of starting materials. The amount of core present in microcapsules was determined by extraction of ALK. To evaluate of microcapsules, a known weight of microcapsules was crushed with pestle and mortar. As a result of crashing, walls of microcapsules were broken down and core washed in the ethanol. After dissolving of the core in the solvent, the shell was filtered, washed with ethanol several times and dried at 40  $^{\circ}\text{C}$  for 24 h in an oven to calculate core wt%.

$$\%Wt_{\text{core}} = (W_c - W_s) / W_c \times 100 \quad (1)$$

The extracted core content ( $\%Wt_{\text{core}}$ ) was calculated using Eq. (1), where  $W_c$  refers to the weight of microcapsules and  $W_s$  refers to the weight of the shell. The core dissolved in ethanol was extracted by the

evaporation method and collected for further analysis.

#### 2.3.3. Morphological studies

**2.3.3.1. Optical microscopy.** The dried products (microcapsules) were all analyzed using an optical microscope (HP model PL20, China) equipped with measuring software (View & Digimizer). It allowed observation of the capsule shape and the approximate size of capsules. For the capsules inspection in different sizes, the dried capsules powder were dispersed on a microscope slide without coverslip and size of capsule subsequently measured using different lenses from 4, 10, 40 and 100x magnification. The size distribution curves were achieved by at least 85 measurements at different magnifications, and the curves were plotted using Minitab software.

**2.3.3.2. Scanning electron microscopy.** The morphology of the microcapsules was also evaluated by a SEM microscope (Philips XL30). SEM analyses were performed at room temperature, and all samples were coated with a layer of gold in vacuum before observing microscopy.

#### 2.3.4. Thermal gravimetric analysis (TGA)

Thermal properties of prepared microcapsules, ALK and PMUF, were analyzed using a thermo gravimetric analyzer (Perkin Elmer STA 6000 TGA system) under an argon atmosphere. The heating rate was adjusted at 20  $^{\circ}\text{C}/\text{min}$  at a temperature range between 30 to 700  $^{\circ}\text{C}$ .

## 3. Results and discussion

### 3.1. Synthesis of microcapsules with ALK as the core material

An in situ microencapsulation process involves the shell hydrophilic materials dissolved in the continuous aqueous environment, and the hydrophobic core material forms an oil-in-water-emulsion. Using chemistry of this reaction [13], during the reaction process, deposition of reaction products occurs at the ALK/water interface, or on the other word, on the surface of the ALK droplets. It provides water-insoluble cross-linked shell layer as previously reported [30]. Simultaneously, the same reaction occurs in solution to produce PMUF particles [13].

In this work, the in situ polymerization of melamine resin-formaldehyde started by adding hydrochloric acid and heating up the reactants. Afterward, due to the increase in the molecular weight of PMUF polymer in the suspension, gradually color of reaction medium turned to a milky white suspension slurry. It was as also reported by other researchers [31].

The acidity of the medium, the amount, and ratio of amino resin are

**Table 2**

The composition of microcapsules prepared at different M/U ratios and its effect on the yield (%) and core content.

Sample code	M/U	M (g)	U (g)	Yield (%)	Core content (%)	Appearance of microcapsules
C1	0.04	0.09	2.49	58	45	White and free flowing
*C2	0.08	0.19	2.47	65	55	White and free flowing
C3	0.16	0.39	2.45	53	40	White and free flowing
C4	0.3	0.73	2.43	–	–	Sticky and agglomerated

\* C2 was chosen as the best result.

important factors that determine structure shell and play key roles in the stability of the microcapsules. If the pH is too high or too low, polymerization of methylolureas with each other or with melamine resin will start at an unsuitable time, which does not lead to the formation of core-shell capsules or makes a shell with undesirable properties.

In the initial stages of this research, polyvinyl alcohol (PVA) was used as a surfactant at different concentrations. Unfortunately, the ALK droplets could not stabilize by PVA, the number of capsules formed was not considerable and the results were not satisfactory. This observation can probably be explained by doing reaction between hydroxyl groups in ALK and PVA structures. After testing some emulsifiers, finally, we decided to use SDBS.

### 3.2. Impact of selected parameters on yield of reaction, core content and microcapsules size

#### 3.2.1. Effect of melamine resin (Cymel 303<sup>®</sup>)/urea ratio

In this section, the effect of changing melamine resin/urea ratio was investigated. As Table 2 displays, PMUF/ALK microcapsules were synthesized with M/U ratio in the range of 0.04–0.3. Results show that with increasing amount of melamine resin, at M/U ratio of 0.08 (sample \*C2 in Table 2), the yield of the product increased up to 65%. Although, a further increase in M/U ratio to 0.16 in sample C3 led to a lower yield of encapsulation i.e. 53%. Higher quantities of melamine resin led to form more agglomerated particles and consequently lower yield. N. Shahabudin et al. also reported similar result [13]. It is probably attributed to the increasing reactions between excessive amounts of M and urea-formaldehyde (methylol) pre-polymer from one side and with ALK on the other side [29]. Fig. 3 illustrates a possible reaction between ALK and the methylated group of M.

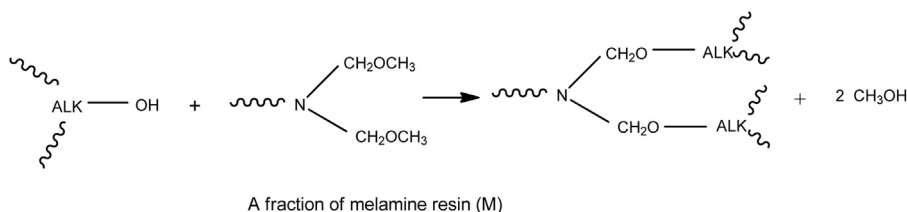
#### 3.2.2. Effect of initial pH value of medium reaction and agitation rate

The effect of initial pH and agitation rate on yield of encapsulation reaction are summarized in Table 3. Samples in Table 3 were designed according to the best results from Table 2. On the other word, component ratios in Table 3 were adjusted according to \*C2, and to investigate and optimize the encapsulation yield and core content, only the initial pH and agitation rate were changed. It revealed that the PMUF/ALK microcapsules prepared at four different initial pH values which were set at 3.0, 3.3, 3.6 and 3.8. In these series of tests, microcapsule formation at pH value 3.0 was not successful and as Fig. 4a shows, only oily and bulky lumps were obtained. While at pH 3.3 microcapsules were formed, but there was a lot of residual material (PMUF) next to the microcapsules (Fig. 4b) and caused to obtain less yield. At this pH, filtration of the product was also difficult due to the

presence of PMUF particles. Results reported by Rochmadi and Hasakowati also suggested that at pH value lower than 3.5 leads to the formation of more PMUF nanoparticles that attached to the microcapsule surface to build a thicker capsule shell and also in the medium reaction [32]. To reduce undesirable PMUF particles in suspension, and for completing of polycondensation reaction at interface ALK/water, pH value increased to 3.6. Fig. 4c shows the formation of microcapsules when using the optimized pH value i.e. 3.6. It exhibits solitary round microcapsules whereas, in this pH, the encapsulation yield was acquired in the highest amount (65%) comparing to the rest experiments in this series. Eventually, a slightly less acidic pH i.e. 3.8 resulted in the production of in many microcapsules, although, they were agglomerated and sticky densely packed together and was not possible to separate them by further washing using different solvents (Fig. 4d). The main reason is that when pH increased, the particle size is decreased and the capsule shells become smoother due to the absence of deposition of PMUF particles on the surface of shells. Zhou et al. studied the effect of the pH value on the formation of UF microcapsules. He concluded a high pH value greater than 3.0 prevents the deposition of UF nanoparticles onto the surface of the microcapsule [33]. This phenomenon is also confirmed by results obtained by Cosco et al. [34,35].

During synthesis, microcapsules size controlled by the agitation rate. In this research, agitation rate of above 450 rpm led to deposition of the PMUF and ALK on the reactor's wall and the stirrer, resulting in a very low yield. We could not measure the yield as separation of microcapsules was very difficult to for further investigations. In fact, a collision between ALK droplets (at a very high stirring rate higher than 450 rpm) occurs which leads to the formation of sticky and oily agglomerated microcapsules. It is presumably due to capsule rupture and thus reduced encapsulation yield. Fig. 5 shows part of a ruptured microcapsule. In this test series, the rupturing of microcapsules occurred more likely, when the speed of stirrer was faster than 450 rpm. This result is in agreement with the results reported by Chen et al. [36].

Therefore, agitation rates of 350 and 450 rpm were selected which led to the formation of capsules with the diameter ranging from approximately 1–40 micrometers (Fig. 6). According to the mentioned figure, as the agitation rate decreases from 450 to 350 rpm, (samples P2, \*P3 to P5, P6) the mean diameter of microcapsules increases. Regarding Table 3, samples P2 and P3 produced microcapsules at higher yield as well. On the other word, with reducing the agitation rate, the bigger ALK droplets were produced, and the formaldehyde and urea would be in excess amounts, compared with ALK. This event led to formation more agglomerated residues (PMUF) and caused to the reduction of yield. These results are by the results reported by others

**Fig. 3.** Possible reaction of ALK with methylated group of M.



**Table 3**

Effect of initial pH and agitation rates on yield (%) of encapsulation reaction and core content.

Sample code	Initial pH	Agitation rate (rpm)	Yield (%)	Core content (%)	Appearance of microcapsules
P1	3	450	–	–	No capsule
P2	3.3	450	58	52	White and free flowing with a lot of residual material
P3	3.6	450	65	55	White and free flowing
P4	3.8	450	–	–	Very sticky and agglomerated capsules
P5	3.3	350	44	45	Free flowing with a lot of residual material
P6	3.6	350	55	50	Free flowing with a lot of residual material

Component ratios were adjusted according to \*C2, as the best result.

\* P3 was chosen as the best result for characterizations.

[2,3,33,37,38].

### 3.3. Characterizations of microcapsules and verification of core content determined by FTIR spectroscopy

Fig. 7 displays the overlaid spectra of the microcapsules (spectrum a), sample \*P3, PMUF (spectrum b), shell material, the ALK (spectrum c), core, and extracted core (spectrum d) material from sample \*P3. The spectrum (b) shows the characteristic peaks of the shell with peaks at 1530 and 1637  $\text{cm}^{-1}$  corresponding to C–N and N–H bending, respectively. All characteristic absorptions of PMUF are visible in spectrum such as the N–H, H–C–H, and HN–CO–NH stretching vibrations at 3338  $\text{cm}^{-1}$ , 2948  $\text{cm}^{-1}$ , and 1645  $\text{cm}^{-1}$ , respectively.

Characteristic bands of ALK (Fig. 7c) are observed at 1750  $\text{cm}^{-1}$  for ester groups and small twin peaks at 1604, and 1583  $\text{cm}^{-1}$  shows C=C stretching vibration of the aromatic ring originated from phthalate groups that formed the alkyd resin (as shown in the plausible structure of the alkyd resin in Fig. 1). Also, the aromatic =C–H bending arising from this aromatic functional group appears at 711  $\text{cm}^{-1}$  as a sharp peak. The broad stretching bands at 3450–3650  $\text{cm}^{-1}$  confirm the



Fig. 5. Part of a microcapsule ruptured at agitation rate above 450 rpm using optical microscopy.

presence of free hydroxyl and carboxyl groups, while the peaks at 2850 and 2949  $\text{cm}^{-1}$  are due to C–H stretching aliphatic. Peaks are also observed at 1050–1280  $\text{cm}^{-1}$  for C–O–C stretching of ester support

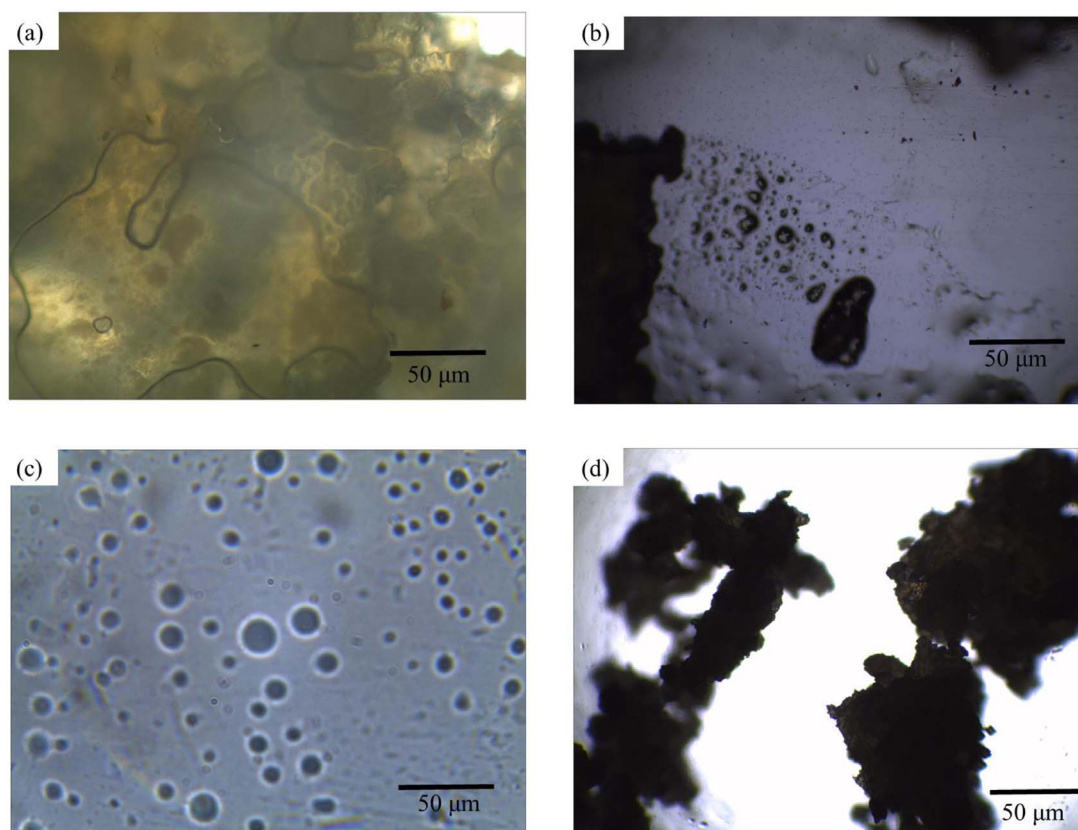


Fig. 4. Optical microscopic images of PMUF/ALK microcapsules prepared in the same agitation rate and at various initial pH-values: (a) pH 3.0, (b) pH 3.3, (c) pH 3.6, and (d) 3.8.

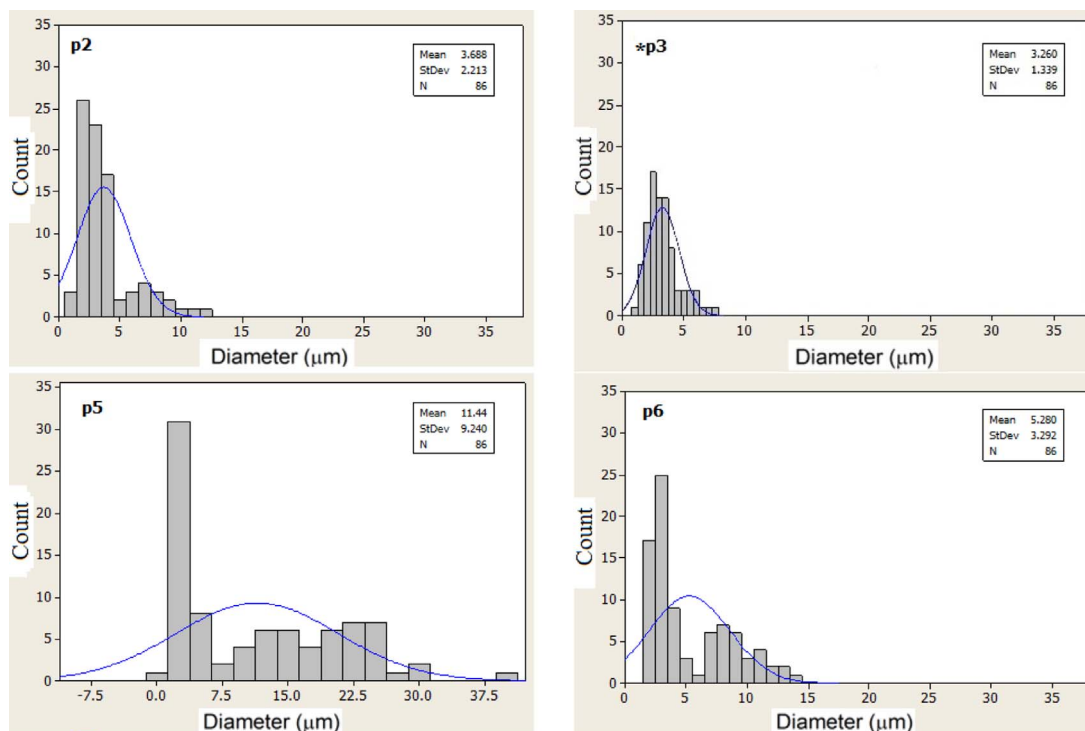


Fig. 6. Size distribution of microcapsules, prepared under different agitation rates and pH values.

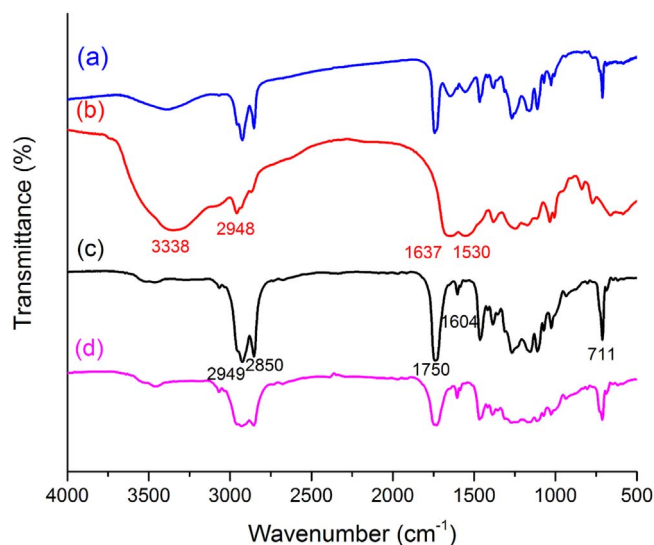


Fig. 7. FTIR spectra of (a) microcapsules (sample \*P3); (b) PMUF (shell material); (c) ALK (core); and (d) extracted core material from sample \*P3.

the structure of ALK. A close matching between spectra of ALK and microcapsules was also found at characteristic peaks for C=O, C–H stretching vibrations and aromatic =C–H bending phthalate units. Given these observations, it is established that ALK was successfully encapsulated by melamine PMUF resin. Also, FTIR spectra of neat ALK and extracted core material are indicated in Fig. 7d, which have been found matching that confirms core material is based on ALK. In other words, encapsulation process has not made any change in molecular structure of the core.

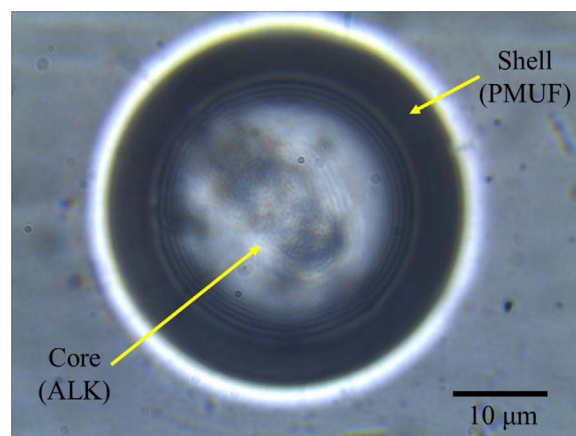


Fig. 8. An optical microscope image of sample P5.

### 3.4. Morphological studies

#### 3.4.1. Shape and size distribution of microcapsules determined by optical microscopy

Fig. 8 shows an optical microscope image of one microcapsule chosen from sample P5 (with the biggest diameter, 40 μm). It is clearly shown that the microcapsule is spherical, a solid polymeric shell (PMUF) and a liquid core material (ALK), as their structures were confirmed by FTIR results. The spherical shape of microcapsules guarantees easy dispersion into the coating before applying. According to optical theory, two different refractive index media microencapsulate each other, the diffraction ring will occur at the interface between the two different media, as also reported in previous work [28]. This diffraction ring also observed in prepared PMUF microcapsules, as the black loop area (the shell wall material) indicating that the shell successfully encapsulates core.

To ensure uniform size distribution of synthesized microcapsules, size distributions of microcapsules were determined using an optical microscope, and as expected, the diameter of synthesized microcapsules

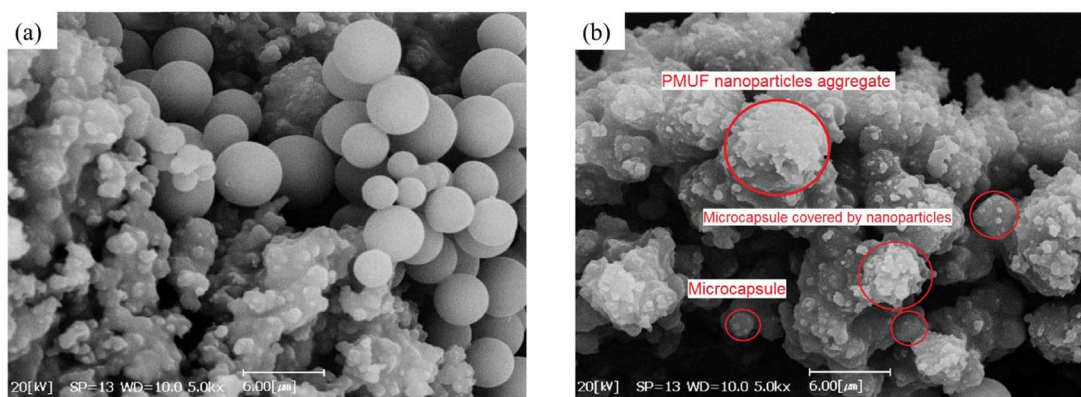


Fig. 9. SEM micrographs of microcapsule sample \*P3 obtained at different locations (a & b).

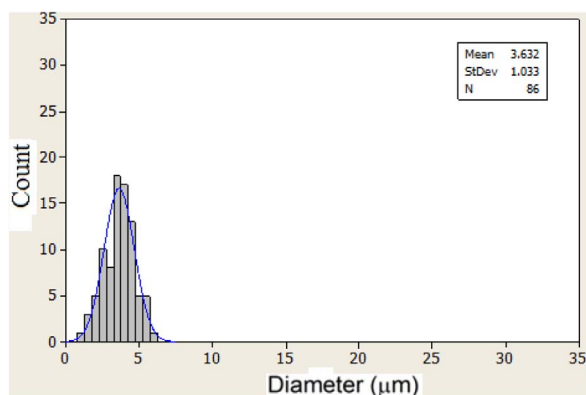


Fig. 10. Size distribution of ALK filled microcapsules \*P3 obtained from SEM images.

was different. Fig. 6 shows size distribution of microcapsules which synthesized at two different agitation rates and pH values. As shown in the figure the mean diameter of the polydispersed microcapsules decreased from 11.44  $\mu\text{m}$  (pH = 3.3) and 5.280  $\mu\text{m}$  (pH = 3.6) to 3.688  $\mu\text{m}$  (pH = 3.3) and 3.260  $\mu\text{m}$  (pH = 3.6) as the agitation rate was increased from 350 to 450 rpm. The reason for this wide size distribution is that the fluid flow around the propeller is turbulent. In the area of flow away from the propeller, many larger micro eddies exist, on the other hand, in the adjacency of propeller blades, many smaller micro eddies exist, which result in a broader length scale as this fact also reported by another researcher [39].

### 3.4.2. Scanning electron microscope (SEM)

Fig. 9 presents SEM micrographs of microcapsule sample \*P3 taken at two different locations of the sample. The variation in diameter and surface of the microcapsules can be noticed. Fig. 9a shows some

individual microcapsules. By looking at Fig. 9b, it is clearly observed that the surface of microcapsules are rough and irregular, and it is composed of PMUF nanoparticles protruding from the surface. When the ratio of the F to U is higher, the condensation reaction rate increases, which results in fast deposition of PMUF nanoparticle on the surface of microcapsules. This phenomenon led to creating rough and jagged outer layer of PMUF shell. The same results were reported in previous researches [28,38]. The gibbous nanoparticles can provide the additional interfacial area necessary for microcapsules and might help for better adhesion to the matrix film. [40]. This presumably eases the fracture of microcapsules due to stress generated in the scribed area. Furthermore, Fig. 10 shows size distribution of ALK filled microcapsules \*P3 obtained from SEM images. Mean diameter of microcapsules was determined to be 3.63  $\mu\text{m}$ , which is very close and is in good agreement with results mean diameter of microcapsules for sample \*P3 obtained by optical microscopy (Fig. 6).

### 3.5. Thermal stability of microcapsules

Thermogravimetry analysis was carried out for thermal degradation characterization of the microcapsules (sample \*P3). Fig. 11 shows TGA and derivative thermogravimetric analysis (DTGA) curves of neat ALK as well as the core/shell microcapsules and PMUF shell.

The ALK was thermally stable up to 282  $^{\circ}\text{C}$  and subsequently decomposed completely at one stage around 520  $^{\circ}\text{C}$ . In curves (II) and (III), the first decompositions were observed at under 100  $^{\circ}\text{C}$  which attributed to the evaporation of water and free formaldehyde. The shell material was thermally stable up to  $\sim 205$   $^{\circ}\text{C}$ , degradation of PMUF occurred in two stages, the first stage at 205–308  $^{\circ}\text{C}$  and the second stage from 308 up to 600  $^{\circ}\text{C}$ . Microcapsules thermal decomposition started around 205  $^{\circ}\text{C}$  and continued up to 308  $^{\circ}\text{C}$ . This was attributed to the degradation of PMUF resin (Shell) that formaldehyde would be partially removed above 200  $^{\circ}\text{C}$ . The second stage of decomposition

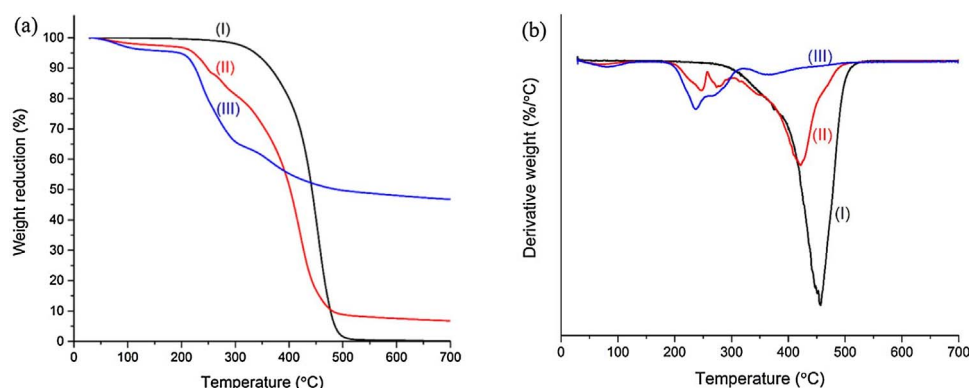


Fig. 11. (a) TGA and (b) DTGA curves for (I) ALK (core); (II) Microcapsules (sample \*P3) and (III) PMUF (shell).



occurred between 308 and 520 °C which is due to decomposition of ALK encapsulated in the shell. The thermal degradations of the core and shell have taken place in overlapping temperature range (~205–520). From these results, it is further established that microcapsules contain both materials, i.e. ALK (as core) and PMUF resin (as shell).

#### 4. Conclusions

A coconut oil-based alkyd resin has been satisfactorily encapsulated in the PMUF shell via an in-situ polymerization using sodium dodecyl benzene sulfonate as an emulsifier. Results obtained in this study revealed significance effects of M/U ratio, initial pH value of the reaction medium, and agitation rate on encapsulation process. The white, free-flowing microcapsules achieved by optimizing conditions at M/U ratio of 0.08, initial pH value 3.6 and agitation rate of 450 rpm. According to this research, the mean diameter of the polydispersed microcapsules decreased as the agitation rate was increased. At these circumstances, spherical microcapsules with diameters in the range of 1–40 µm were prepared, whereas the yield of encapsulation and core content increased up to 65% and 55% respectively. The prepared microcapsules in aforementioned condition are thermally stable just below 205 °C. The SEM images from the optimized sample disclosed that the outer surfaces of microcapsules are rough due to agglomerated PMUF nanoparticles, which is desirable. In general, this research provides microcapsules filled by ALK for the self-healing purposes, and the effects of the microcapsules on the epoxy matrix will be further examined in our future study.

#### References

- [1] M. Zheludkevich, Self-healing anticorrosion coatings, *Self-Healing Materials*, Wiley-VCH Verlag GmbH & Co. KGaA, 2009, pp. 101–139.
- [2] E.N. Brown, M.R. Kessler, N.R. Sottos, S.R. White, In situ poly (urea-formaldehyde) microencapsulation of dicyclopentadiene, *J. Microencapsulation* 20 (2003) 719–730.
- [3] B. Blaiszik, M. Caruso, D. McIlroy, J. Moore, S. White, N. Sottos, Microcapsules filled with reactive solutions for self-healing materials, *Polymer* 50 (2009) 990–997.
- [4] C. Suryanarayana, K.C. Rao, D. Kumar, Preparation and characterization of microcapsules containing linseed oil and its use in self-healing coatings, *Prog. Org. Coat.* 63 (2008) 72–78.
- [5] M. Samadzadeh, S.H. Boursa, M. Peikari, A. Ashrafi, M. Kasirha, Tung oil: an autonomous repairing agent for self-healing epoxy coatings, *Prog. Org. Coat.* 70 (2011) 383–387.
- [6] F. Ahangaran, A.H. Navarchian, M. Hayaty, K. Esmailpour, Effect of mixing mode and emulsifying agents on micro/nanoencapsulation of low viscosity self-healing agents in polymethyl methacrylate shell, *Smart Mater. Struct.* 25 (2016) 095035.
- [7] R.E. Neisiany, S.N. Khorasani, J. Kong Yoong Lee, S. Ramakrishna, Encapsulation of epoxy and amine curing agent in PAN nanofibers by coaxial electrospinning for self-healing purposes, *RSC Adv.* 6 (2016) 70056–70063.
- [8] R.E. Neisiany, J.K.Y. Lee, S.N. Khorasani, S. Ramakrishna, Self-healing and interfacially toughened carbon fibre-epoxy composites based on electrospun core-shell nanofibres, *J. Appl. Polym. Sci.* 134 (2017) 44956.
- [9] Y.C. Yuan, X.J. Ye, M.Z. Rong, M.Q. Zhang, G.C. Yang, J.Q. Zhao, Self-healing epoxy composite with heat-resistant healant, *ACS Appl. Mater. Interfaces* 3 (2011) 4487–4495.
- [10] Y. Zhu, X.J. Ye, M.Z. Rong, M.Q. Zhang, Self-healing glass fiber/epoxy composites with polypropylene tubes containing self-pressurized epoxy and mercaptan healing agents, *Compos. Sci. Technol.* 135 (2016) 146–152.
- [11] F. Ahangaran, M. Hayaty, A.H. Navarchian, Morphological study of polymethyl methacrylate microcapsules filled with self-healing agents, *Appl. Surf. Sci.* 399 (2017) 721–731.
- [12] N. Shahabudin, R. Yahya, S.N. Gan, Microencapsulation of a palm oil-based alkyd by amino resins, *Macromolecular Symposia*, Wiley Online Library, 2015, 2017, pp. 305–313.
- [13] N. Shahabudin, R. Yahya, S.N. Gan, Microcapsules filled with a palm oil-based alkyd as healing agent for epoxy matrix, *Polymers* 8 (2016) 125.
- [14] F.N. Jones, Alkyd resins, *Ullmann's Encyclopedia of Industrial Chemistry*, Wiley-VCH Verlag GmbH & Co. KGaA, 2000.
- [15] S. Ataei, R. Yahya, S.N. Gan, Fast physical drying high water and salt resistant coatings from non-drying vegetable oil, *Prog. Org. Coat.* 72 (2011) 703–708.
- [16] M.M. Caruso, D.A. Delafuente, V. Ho, N.R. Sottos, J.S. Moore, S.R. White, Solvent-promoted self-healing epoxy materials, *Macromolecules* 40 (2007) 8830–8832.
- [17] N. Dutta, N. Karak, S. Dolui, Alkyd-epoxy blends as multipurpose coatings, *J. Appl. Polym. Sci.* 100 (2006) 516–521.
- [18] A. Issam, A.N. Khizrien, I. Mazlan, Physical and mechanical properties of different ratios of palm oil-based alkyd/epoxy resins, *Polym. Plast. Technol. Eng.* 50 (2011) 1256–1261.
- [19] H.R. Ong, M.M.R. Khan, R. Ramli, R.M. Yunus, Effect of CuO nanoparticle on mechanical and thermal properties of palm oil based alkyd/epoxy resin blend, *Procedia Chem.* 16 (2015) 623–631.
- [20] E.F. Assanvo, P. Gogoi, S.K. Dolui, S.D. Baruah, Synthesis, characterization, and performance characteristics of alkyd resins based on Ricinodendron heudelotii oil and their blending with epoxy resins, *Ind. Crops Prod.* 65 (2015) 293–302.
- [21] P. Gogoi, M. Boruah, C. Bora, S.K. Dolui, Jatropha curcas oil based alkyd/epoxy resin/expanded graphite (EG) reinforced bio-composite: evaluation of the thermal, mechanical and flame retardancy properties, *Prog. Org. Coat.* 77 (2014) 87–93.
- [22] S.Y. Lee, S.N. Gan, A. Hassan, K. Terakawa, T. Hattori, N. Ichikawa, D.H. Choong, Reactions between epoxidized natural rubber and palm oil-based alkyds at ambient temperature, *J. Appl. Polym. Sci.* 120 (2011) 1503–1509.
- [23] Y.K. Khong, S.N. Gan, Blends of phthalic anhydride-modified palm stearin alkyds with high carboxylic acid contents with epoxidized natural rubber, *J. Appl. Polym. Sci.* 130 (2013) 153–160.
- [24] X. Liu, X. Sheng, J.K. Lee, M.R. Kessler, Synthesis and characterization of melamine-urea-formaldehyde microcapsules containing ENB-based self-healing agents, *Macromol. Mater. Eng.* 294 (2009) 389–395.
- [25] X.-M. Tong, T. Zhang, M.-Z. Yang, Q. Zhang, Preparation and characterization of novel melamine modified poly (urea-formaldehyde) self-repairing microcapsules, *Coll. Surf. A* 371 (2010) 91–97.
- [26] M.P. Stevens, *Polymer Chemistry: an Introduction*, oxford university press, New York, 1999.
- [27] S. Then, G.S. Neon, A. Kasim, N. Hayaty, Performance of melamine modified urea-formaldehyde microcapsules in a dental host material, *J. Appl. Polym. Sci.* 122 (2011) 2557–2562.
- [28] D.Y. Zhu, M.Z. Rong, M.Q. Zhang, Self-healing polymeric materials based on microencapsulated healing agents: from design to preparation, *Prog. Polym. Sci.* 49 (2015) 175–220.
- [29] J. Orsavova, L. Misurcova, J.V. Ambrozova, R. Vicha, J. Mlecek, Fatty acids composition of vegetable oils and its contribution to dietary energy intake and dependence of cardiovascular mortality on dietary intake of fatty acids, *Int. J. Mol. Sci.* 16 (2015) 12871–12890.
- [30] T. Yin, M.Z. Rong, M.Q. Zhang, G.C. Yang, Self-healing epoxy composites—preparation and effect of the healant consisting of microencapsulated epoxy and latent curing agent, *Compos. Sci. Technol.* 67 (2007) 201–212.
- [31] L. Yuan, G. Liang, J. Xie, L. Li, J. Guo, Preparation and characterization of poly (urea-formaldehyde) microcapsules filled with epoxy resins, *Polymer* 47 (2006) 5338–5349.
- [32] A.P. Rochmadi, W. Hasokowati, Mechanism of microencapsulation with urea-formaldehyde polymer, *Am. J. Appl. Sci.* 7 (2010) 739–745.
- [33] H. Lee, S. Lee, I. Cheong, J. Kim, Microencapsulation of fragrant oil via in situ polymerization: effects of pH and melamine-formaldehyde molar ratio, *J. Microencapsulation* 19 (2002) 559–569.
- [34] S. Cosco, V. Ambrogio, P. Musto, C. Carfagna, Urea-formaldehyde microcapsules containing an epoxy resin: influence of reaction parameters on the encapsulation yield, *Macromolecular Symposia*, Wiley Online Library, 2006, 2017, pp. 184–192.
- [35] S. Cosco, V. Ambrogio, P. Musto, C. Carfagna, Properties of poly (urea-formaldehyde) microcapsules containing an epoxy resin, *J. Appl. Polym. Sci.* 105 (2007) 1400–1411.
- [36] M. Chen, J. Liu, Y. Liu, C. Guo, Z. Yang, H. Wu, Preparation and characterization of alginate-N-2-hydroxypropyl trimethyl ammonium chloride chitosan microcapsules loaded with patchouli oil, *RSC Adv.* 5 (2015) 14522–14530.
- [37] S. Alexandridou, C. Kiparissides, Production of oil-containing polyterephthalamide microcapsules by interfacial polymerization. An experimental investigation of the effect of process variables on the microcapsule size distribution, *J. Microencapsulation* 11 (1994) 603–614.
- [38] H.S. Tan, T.H. Ng, H.K. Mahabadi, Interfacial polymerization encapsulation of a viscous pigment mix: emulsification conditions and particle size distribution, *J. Microencapsulation* 8 (1991) 525–536.
- [39] L. Dobetti, V. Pantaleo, Application of a hydrodynamic model to microencapsulation by coacervation, *J. Microencapsulation* 19 (2002) 139–151.
- [40] G. He, N. Yan, <sup>13</sup>C NMR study on structure, composition and curing behavior of phenol-urea-formaldehyde resole resins, *Polymer* 45 (2004) 6813–6822.